

Generic Contrast Agents

Our portfolio is growing to serve you better. Now you have a *choice*.



[VIEW CATALOG](#)

AJNR

Identification of the Normal Jugular Foramen and Lower Cranial Nerve Anatomy: Contrast-Enhanced 3D Fast Imaging Employing Steady-State Acquisition MR Imaging

I. Davagnanam and S.V. Chavda

This information is current as of May 10, 2025.

AJNR Am J Neuroradiol 2008, 29 (3) 574-576

doi: <https://doi.org/10.3174/ajnr.A0860>

<http://www.ajnr.org/content/29/3/574>

Identification of the Normal Jugular Foramen and Lower Cranial Nerve Anatomy: Contrast-Enhanced 3D Fast Imaging Employing Steady-State Acquisition MR Imaging

TECHNICAL NOTE

I. Davagnanam
S.V. Chavda

SUMMARY: Conventional imaging protocols are unable to visualize the intraforaminal/canalicular segments of the lower cranial nerves (IX–XII). On the basis of previous successful demonstration of individual cranial nerves within the cavernous sinus by constructive interference in steady-state MR imaging, we describe the use of contrast-enhanced 3D fast imaging employing steady-state acquisition MR imaging to demonstrate normal in vivo intraforaminal and canalicular segments of cranial nerves IX–XII in 10 patients by using a standardized imaging protocol.

The detection of individual cranial nerves in the intraforaminal portion of the jugular foramen and hypoglossal canal is useful in diagnostic imaging¹; however, visualization by using conventional MR imaging protocols does not provide adequate detail of individual nerves.^{2,3} Recently, contrast-enhanced 3D constructive interference in steady state (CISS) MR imaging has successfully demonstrated the trigeminal ganglion and its divisions and individual cranial nerves within the cavernous sinus.^{4,5} 3D fast imaging employing steady-state acquisition (FIESTA) is a similar form of steady-state sequence MR imaging. Evidence has shown a proportional increase in contrast between the background structures and the cranial nerves within the cisterns as the concentration of gadolinium-based contrast agent increases with 3D steady-state imaging sequences.^{4,6}

This Technical Note describes the use of 3D-FIESTA imaging after intravenous administration of gadodiamide hydrate contrast to demonstrate the normal anatomy of the intraforaminal and canalicular portions of cranial nerves IX–XII.

Description of the Technique

Detectability of the intraforaminal/canalicular segments of cranial nerves IX–XII was evaluated in 10 consecutive patients undergoing routine follow-up imaging for vestibular schwannomas. Patients included 6 men and 4 women (mean age, 56.8; range, 36–68 years).

MR Imaging

The examinations were performed on a 1.5T unit (Signa Excite HD; GE Healthcare, Bucks, UK) with a standard head coil and pre- and postcontrast enhancement with a standardized FIESTA MR imaging protocol. Gadodiamide hydrate (Omniscan; GE Healthcare) was administered at 0.1-mmol/kg body weight as an intravenous contrast agent. The pulse sequence used was the following: 3D FIESTA-C (TR/TE/NEX, 5.5/1.7/3.00; 180 × 180 mm [read x phase encode] FOV;

0.4-mm effective section thickness; 448 × 448 matrix; and imaging time of 8 minutes 21 seconds).

Image Analysis

The datasets obtained were reconstructed in the 3 orthogonal/oblique planes in relation to the cisternal course of the cranial nerves. Images were viewed on high-resolution monitors with a multiplanar reconstruction program (Advantage Workstations; GE Healthcare).

The initial evaluation involved an assessment of the division of the jugular foramen into the pars nervosa and pars vascularis, separated by the fibrous or bony septum (jugular ligament) represented by a dark line (Fig 1). A further attempt was then made to identify cranial nerves IX–XII within the jugular foramen and hypoglossal canal, appearing as hypointense bands or spots. The continuity of nerves was confirmed by tracking their courses proximal and distal to the skull base on >3 consecutive sections in the reconstructed planes to distinguish these from other structures and artifacts, thereby reducing false-positives. Comparison with the precontrast images was then undertaken after identification of cranial nerves on the postcontrast images. This process averaged 26 minutes (range, 18–35) per patient to reconstruct, analyze, and correlate the imaging with the anatomic course of lower cranial nerves.

The images were evaluated by 2 neuroradiologists, making initial evaluations independently but resolving any inconsistencies by collaborative review and consensus agreement.

Results

There was consensus agreement that enhancement of the jugular vein and associated venous plexus surrounding the cranial nerves provided excellent contrast of the small structures within the jugular foramen on FIESTA images, unlike on precontrast FIESTA (Fig 2) and standard imaging sequences.

The jugular ligament was identified on the contrast-enhanced sequence in all 20 jugular foramina. The intraforaminal and canalicular segments of cranial nerves IX–XII were localized in all cases consistent with the known anatomic courses of cranial nerves IX–XII (Fig 3). Disagreement between observers relating to the identification of the spinal roots of the accessory nerve (XI) occurred in 2 cases but was resolved by consensus review and agreement.

Discussion

As early as 1985, Daniels et al⁷ attempted to correlate the course of cranial nerves IX through XI in cadaveric specimens

Received August 1, 2007; accepted August 2.

From the Department of Neuroradiology, University Hospital Birmingham, Birmingham, UK. Paper previously presented at: Annual Meeting of the American Society of Head and Neck Radiology, September 27, 2006, Phoenix, Ariz; Annual Meeting of the International Congress of Head and Neck Radiology, September 29, 2006, Budapest, Hungary; and Royal Society of Medicine, London, UK, for the Finzi Prize, November 24, 2006.

Please address correspondence to Indran Davagnanam, MD, Department of Neuroradiology, University Hospital Birmingham, Queen Elizabeth Medical Centre, Birmingham B15 2TH, UK; e-mail: indran_davagnanam@yahoo.co.uk

DOI 10.3174/ajnr.A0860

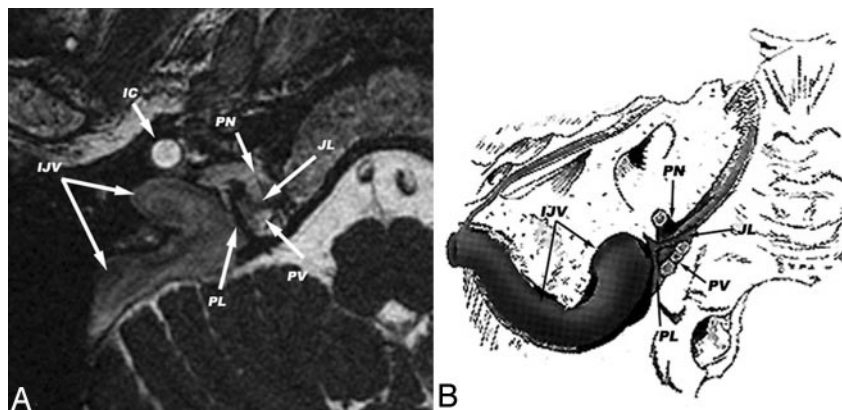


Fig 1. Axial postcontrast FIESTA acquisition through the jugular foramen (A) and a diagrammatic representation of the corresponding axial section (B) (adapted from Leblanc A. *The Cranial Nerves: Anatomy-Imaging-Vascularization*. 2nd ed. Berlin, Germany: Springer; 1996) showing the following: opacified internal jugular vein (IJV), internal carotid artery (IC), jugular ligament (JL), petro-occipital ligament (PL), and division of the pars nervosa (PN) from the pars vascularis (PV).

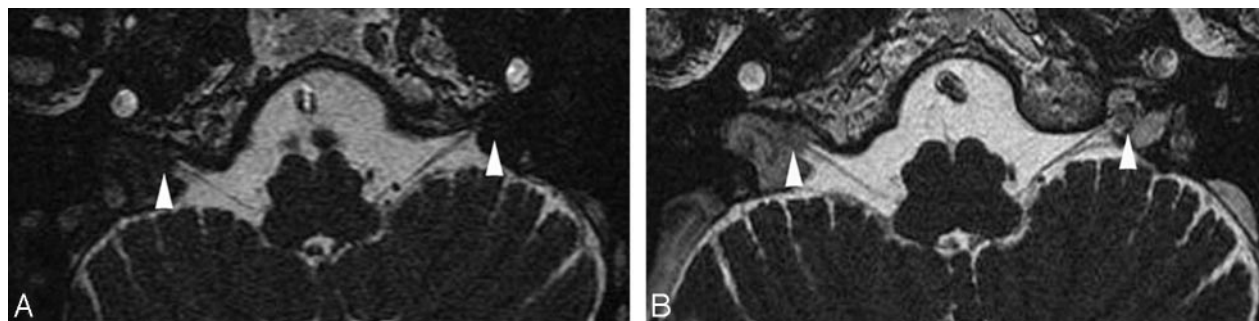


Fig 2. Axial pre- (A) and postgadolinium (B) FIESTA acquisitions showing the length of the vagus nerve (X) bilaterally. The images were windowed at comparable levels (C:3886, W:12,502) demonstrating the effect of enhancement of the venous plexus adjacent to the intraforaminal segment of the cranial nerves (arrowheads).

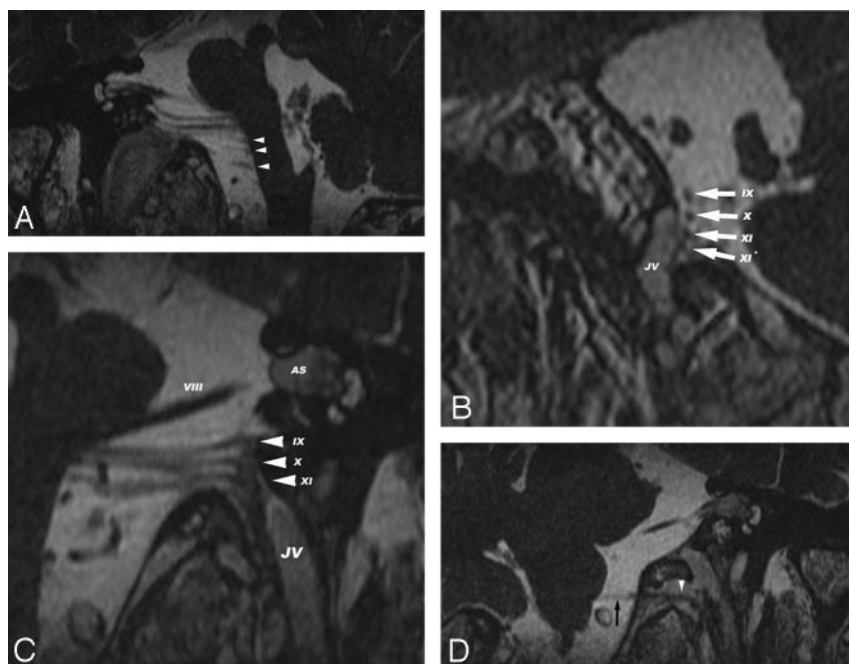


Fig 3. Postgadolinium FIESTA acquisitions reformatted in the following planes: the coronal-oblique plane demonstrating the spinal roots of the accessory nerve (XI) (A, white arrowheads); the sagittal-oblique plane demonstrating the intraforaminal segments (B, white arrows) of the glossopharyngeal (IX), vagus (X), cranial accessory (XI), and spinal accessory (XI*) nerves adjacent to the opacified jugular vein (JV); the coronal-oblique plane demonstrating a left vestibular schwannoma (AS) of the vestibulocochlear nerve (VIII) and the intraforaminal segments (C, white arrowheads) of the glossopharyngeal (IX), vagus (X), and cranial accessory (XI) nerves adjacent to the opacified jugular vein (JV); and the coronal-oblique plane demonstrating the cisternal course (D, black arrow) and intracanalicular segment (D, white arrowhead) of the hypoglossal nerve (XII).

with standard 1.5T MR imaging. With the advent of steady-state imaging, the use of uncontrasted CISS/FIESTA sequences have become an integral part of the assessment of pathology involving the cranial nerves VII and VIII (particularly vestibular schwannomas).^{6,8} In 2001, Seitz et al² suggested a combination of 3D CISS and magnetization-preparation rapid gradient-echo imaging, where the 2D technique had failed to demonstrate lower cranial nerves. Its utility had been extended in the successful demonstration of the visualization

of microvascular compression of cranial nerve IX in glossopharyngeal neuralgia⁹ and the cochlear nerve in presurgical cochlear-implant candidates (high-field 3T).¹⁰

The steady-state sequence depicts small structures surrounded by CSF with high contrast and spatial resolution, using a refocused gradient-echo sequence. This uses a phase-cycling technique and a steady-state contrast mechanism to provide high signal intensity-to-noise ratio images with heavy T2-weighted signal intensity while suppressing background

tissue. The sequences are extremely short (TR) between radio-frequency pulses, such that high-resolution 3D volume images can be acquired rapidly.¹¹ The jugular ligament and intraforaminal/canalicular segments of cranial nerves IX–XII were consistently and distinctly demonstrated in all our patients with this technique. This was further facilitated by enhancement of the adjacent jugular vein and venous plexus, resulting in an increase in contrast between cranial nerves and the background, similar to that previously described within the cisterns.^{4–6}

The application of contrast-enhanced steady-state imaging has recently successfully delineated cranial nerves in the cavernous sinus⁴ as well as the trigeminal ganglion and its motor and sensory divisions.⁵ To our knowledge, assessment by contrast-enhanced steady-state MR imaging has, however, never been performed to visualize the intraforaminal/canalicular segments of the lower cranial nerves before this study.

The identification of normal cranial nerves may have implications in determining the involvement by pathologic processes as well as for neural preservation surgery of tumors in this region.¹² However, the authors acknowledge that the variability in the course of the cranial nerves within the jugular foramen may hinder the full utility of this technique.

Conclusion

The reproducibility and consistency in demonstrating the distinct anatomic courses of cranial nerves IX–XII of contrast-enhanced 3D-FIESTA MR imaging in vivo makes this technique potentially useful in the evaluation of the extent of cranial nerve involvement by tumors. It can be more accurately compared with traditional combinations of clinical symptoms, standard CT, and MR imaging and is useful in

planning before biopsy and neural preserving surgical procedures.

References

1. Eldevik OP, Gabrielsen TO, Jacobsen EA. **Imaging findings in schwannomas of the jugular foramen.** *AJNR Am J Neuroradiol* 2000;21:1139–44
2. Seitz J, Held P, Fründ R, et al. **Visualization of the IXth to XIIth cranial nerves using 3-dimensional constructive interference in steady state, 3-dimensional magnetization-prepared rapid gradient echo and T2-weighted 2-dimensional turbo spin echo magnetic resonance imaging sequences.** *J Neuroimaging* 2001;11:160–64
3. Suzuki H, Maki H, Maeda M, et al. **Visualization of the intracisternal angioarchitecture at the posterior fossa by use of image fusion.** *Neurosurgery* 2005;56:335–42
4. Yagi A, Sato N, Taketomi A, et al. **Normal cranial nerves in the cavernous sinuses: contrast-enhanced three-dimensional constructive interference in the steady state MR imaging.** *AJNR Am J Neuroradiol* 2005;26:946–50
5. Yousry I, Moriggl B, Schmid UD, et al. **Trigeminal ganglion and its divisions: detailed anatomic MR imaging with contrast-enhanced 3D constructive interference in the steady state sequences.** *AJNR Am J Neuroradiol* 2005;26:1128–35
6. Shigematsu Y, Korogi Y, Hirai T, et al. **Contrast-enhanced CISS MRI of vestibular schwannomas: phantom and clinical studies.** *J Comput Assist Tomogr* 1999;23:224–31
7. Daniels DL, Schenck JF, Foster T, et al. **Magnetic resonance imaging of the jugular foramen.** *AJNR Am J Neuroradiol* 1985;6:699–703
8. Casselman JW, Kuhweide R, Deimling M, et al. **Constructive interference in steady state-3DFT MR imaging of the inner ear and cerebellopontine angle.** *AJNR Am J Neuroradiol* 1993;14:47–57
9. Karibe H, Shirane R, Yoshimoto T. **Preoperative visualization of microvascular compression of cranial nerve IX using constructive interference in steady state magnetic resonance imaging in glossopharyngeal neuralgia.** *J Clin Neurosci* 2004;11:679–81
10. Lane JJ, Ward H, Witte RJ, et al. **3-T imaging of the cochlear nerve and labyrinth in cochlear-implant candidates: 3D fast recovery fast spin-echo versus 3D constructive interference in the steady state techniques.** *AJNR Am J Neuroradiol* 2004;25:618–22
11. Nitz WR. **Fast and ultrafast non-echo-planar MR imaging techniques.** *Eur Radiol* 2002;12:2866–82
12. Lustig LR, Jackler RK. **The variable relationship between the lower cranial nerves and jugular foramen tumors: implications for neural preservation.** *Am J Otol* 1996;17:658–68